

Optical spectroscopy study on the electronic structure of $\text{Eu}_{1-x}\text{Ca}_x\text{B}_6$

Jungho Kim and S.-J. Oh

*School of Physics Center for Strongly Correlated Materials Research,
Seoul National University, Seoul 151-742, Republic of Korea*

Youngwoo Lee and E. J. Choi*

Department of Physics, University of Seoul, Seoul 130-743, Republic of Korea

C. C. Homes

Department of Physics, Brookhaven National Laboratory, Upton, NY 11973-5000

Jong-Soo Rhyee and B. K. Cho

*Center for Frontier Materials and Department of Materials Science and Engineering,
K-JIST, Gwangju 500-712, Korea*

The optical conductivity $\sigma_1(\omega)$ of $\text{Eu}_{1-x}\text{Ca}_x\text{B}_6$ has been obtained from reflectivity and ellipsometry measurements for series of compositions, $0 \leq x \leq 1$. The interband part of $\sigma_1(\omega)$ shifts continuously to higher frequency as Ca-content x increases. Also the intraband spectral weight of $\sigma_1(\omega)$ decreases rapidly and essentially vanishes for $x \geq x_c = 0.35$. These results show that the valence band and the conduction band of $\text{Eu}_{1-x}\text{Ca}_x\text{B}_6$ move away from each other such that their band overlap decreases with increasing Ca-substitution. As a result, the electronic state evolves from the semimetallic structure of EuB_6 to the insulating CaB_6 where the two bands are separated to open a finite gap ($\simeq 0.25$ eV) at the X-point of the Brillouin zone.

PACS numbers: 71.20.-b, 71.30.+h, 78.20.-e

The divalent hexaboride compounds RB_6 (R=Eu, Ca, Sr, etc) have drawn much attention for the last decade due to their interesting electrical and magnetic properties. These materials crystallize in a cubic structure with boron octahedra in the center of the unit cell and the cations sitting on the corners of the cube. In EuB_6 , the Eu ions ($S = 7/2$) exhibit a ferromagnetic alignment at $T_C = 15$ K.^{1,2} This transition accompanies a large drop of dc-resistivity.³ In addition, the infrared reflectivity measurement showed an unusual shift of the plasma frequency across the transition.⁴ The resistivity and the plasma frequency changes are also induced by external magnetic field.⁵

The hexaboride CaB_6 is isovalent with EuB_6 . However, the low-temperature dc-resistivity exhibits a semi-conducting temperature dependence, in contrast with the metallic behavior of EuB_6 . While the Ca ion bears no magnetic moment, weak ferromagnetism was observed at high temperature ($T_C \sim 600$ K) in the lightly La-doped $\text{Ca}_{1-x}\text{La}_x\text{B}_6$ as well as in the nominally stoichiometric CaB_6 compound.⁶ Various explanations of this effect such as the excitonic state model^{7,8,9,10,11} and the dilute electron gas model^{6,12,13} have been proposed. The effect is also attributed to extrinsic origin such as structural defect or impurities.^{14,15,16,17}

As a prerequisite to the understanding of these unconventional phenomena, the band structure of EuB_6

and CaB_6 were extensively studied both theoretically and experimentally. de Haas-van Alphen (dHvA) and Shubnikov de Hass (SdH) experiments show a semimetallic band structure in both materials, i.e, both electron pocket and hole pocket exist on the Fermi surface.^{18,19,20,21} On the other hand, angle resolved photoemission spectroscopy (ARPES) and soft x-ray emission measurements showed that in both compounds the bands are separated with a sizable gap of ~ 1 eV.²² Theoretically, the early local-density approximation (LDA) band calculation predicted that, in EuB_6 and CaB_6 , conduction band (CB) overlaps with valence band (VB) at X point of the Brillouin zone.²³ LDA+U calculation result for EuB_6 agrees with this semimetallic band structure.²⁴ However, for CaB_6 , pseudo-potential GW^{25,26} and also WDA calculation²⁷ claim an insulating state with a sizable band gap of 0.8 eV. On the contrary, all electron GW calculation by Kino *et al.* shows that CaB_6 does not have such a large gap.²⁸ A full-potential LMTO calculation yields a moderate gap of 0.3 eV.²⁹ This lack of consistency among different results suggests that the band structure depends much on the details of the employed calculation methods.

Recently, Rhyee *et al.* have prepared a series of $\text{Eu}_{1-x}\text{Ca}_x\text{B}_6$ where Eu is gradually replaced by the isovalent Ca.^{30,31} As the Ca-content x increases, the metallic dc-resistivity $\rho(T)$ was found to increase and then crosses over to an insulating behavior. Noting that no carrier doping is expected in this series of isovalent samples, the evident changes of the electrical properties imply a non-trivial effect of the Ca-substitution. Also, this system provides an opportunity to understand, when com-

*To whom all correspondences should be addressed:
echoi@uos.ac.kr.

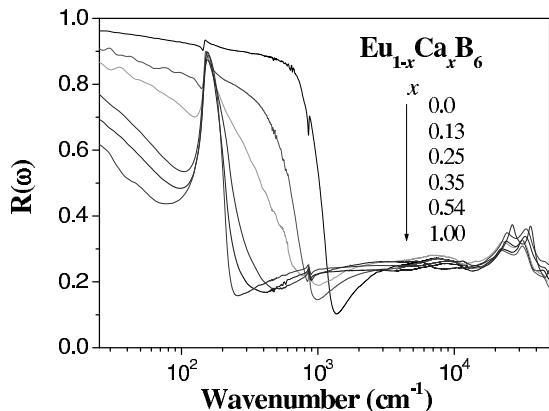


FIG. 1: Reflectivity spectra of $\text{Eu}_{1-x}\text{Ca}_x\text{B}_6$ for various values of x from $x = 0$ (EuB_6) and $x = 1$ (CaB_6) taken at room temperature.

combined with a spectroscopic measurement, how the electronic structure changes along with the cation substitution. This will provide useful clues about the band structure of the two parent compounds EuB_6 and CaB_6 .

In this study, we have performed a wide range ($20 - 50,000 \text{ cm}^{-1}$) optical spectroscopic measurement of $\text{Eu}_{1-x}\text{Ca}_x\text{B}_6$ for a series of compositions x which ranges from 0 to 1. The single-crystal samples were synthesized by a boro-thermal method as described in detail elsewhere.^{30,31} Boron powder of 99.9% purity was used. To determine the Eu content x , we measured the dc-magnetization $M(H)$ of each sample until it saturates at high magnetic field H . The saturation value is proportional to x , from which we find $x = 0, 0.13, 0.25, 0.35, 0.54$ and 1. Dc-resistivity and Hall coefficient of these samples were reported in the earlier publication.³¹ For present optical study, crystals from the same sample batches were used. The reflectance $R(\omega)$ at a near-normal angle of incidence was measured at 300 K in the $20 - 5000 \text{ cm}^{-1}$ and $5000 - 50000 \text{ cm}^{-1}$ ranges using a Fourier transform spectrometer with an *in situ* overcoating technique,³² and a grating spectrometer with a V-W method, respectively. The crystals were wedged by 2° to avoid internal interference effect.

Figure 1 shows the reflectivity of $\text{Eu}_{1-x}\text{Ca}_x\text{B}_6$ over the wide range of frequency. In the low energy infrared region, the spectra exhibit a large change with x . For $x=0$ (EuB_6), $R(\omega)$ is high and shows a plasma edge at $\omega \sim 1,200 \text{ cm}^{-1}$, which is similar to the earlier observation by Degiorgi *et al.*⁴ As x increases, the reflectivity level decreases and the plasma edge shifts continuously toward lower frequency. For $x \geq 0.35$, this metallic feature of $R(\omega)$ is significantly suppressed and the phonon peak at 150 cm^{-1} becomes prominent. The absorption peaks at high energy ($\omega > 10^4 \text{ cm}^{-1}$) correspond to interband excitations.

The real part of the optical conductivity $\sigma_1(\omega)$ has been determined from a Kramers-Kronig analysis of the

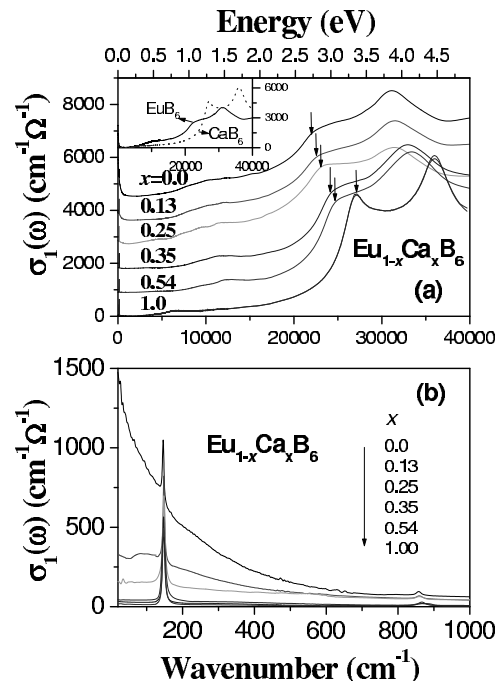


FIG. 2: Optical conductivity $\sigma_1(\omega)$ of $\text{Eu}_{1-x}\text{Ca}_x\text{B}_6$ for: (a) wide-range of frequency up to 5 eV; (b) low-frequency infrared region. In (a), the curves are uniformly displaced along the vertical axis to avoid heavy overlap among them. Inset shows $\sigma_1(\omega)$ of EuB_6 and CaB_6 without the vertical shift.

measured reflectance, for which extrapolations for $\omega \rightarrow 0$ and ∞ must be supplied. For $\omega \rightarrow 0$, the Hagen-Rubens (HR) extrapolation was employed. Above the highest measured frequency, a free-electron approximation $R(\omega) \propto \omega^{-4}$ was assumed. For $1.5 \leq \omega \leq 5.5 \text{ eV}$, an ellipsometer (Sopra GES5) was used to directly determine $\sigma_1(\omega)$. The result showed a good agreement with the reflectance measured in the same region.

Figure 2(a) displays the overall structure of $\sigma_1(\omega)$ on a linear scale. To allow for a clearer presentation, the curves are displaced uniformly along the vertical axis. The conductivity $\sigma_1(\omega)$ consists of a gradual rise up to $\simeq 2.5 \text{ eV}$ and two eminent peaks at 2.7 and 3.7 eV, respectively. Also a weak absorption appears at about 1.5 eV. Note that the 2.7 eV peak shifts to higher energy as x increases, as indicated by the arrows. A similar shift occurs with the 3.7 eV peak as well. The inset displays $\sigma_1(\omega)$ of $x = 0$ and 1 without the vertical displacement. Note that the shift occurs over the wide energy range, including the region of the gradual rise.

We assign the observed $\sigma_1(\omega)$, the rise and the peaks, to interband transitions of $\text{Eu}_{1-x}\text{Ca}_x\text{B}_6$. Band structure calculations show that in EuB_6 , the CB width is about $3 \sim 4 \text{ eV}$ and the band bottom is formed at the X point of the Brillouin zone (BZ). The VB top is located at the same point. Most of the calculations show that, in EuB_6 , the two bands overlap by small amount to form

a semimetallic state.^{23,24} An optical excitation from the VB to the CB will then occur over a broad frequency from $\omega = 0$ to the maximal interband energy. For instance, according to Massidda *et al.*, the 2.75 eV peak corresponds to the VB-CB excitation at the Γ point.²³ The blue shift of $\sigma_1(\omega)$ which occurs nearly uniformly over the wide frequency range implies that with Ca-doping, the VB-CB distance increases throughout the BZ.

In EuB_6 , the VB is formed by the B $2p$ level, while the CB is derived from the hybridization of the cation d (Eu $4d$) and B $2p$ levels.^{23,24,25,26,33} As Ca is introduced, the lattice constant of $\text{Eu}_{1-x}\text{Ca}_x\text{B}_6$ monotonically decreases.³⁰ Also, within the unit cell, the cation-boron distance decreases and as a result, the hybridization will change. In addition, Eu^{+2} has a larger ionic radius than Ca^{+2} (1.12 Å vs 1.0 Å). These structural and chemical changes seem to contribute to the observed band shift. Further, Kuneš *et al.* showed that in EuB_6 , the Eu $4f$ state, through hybridization with B $2p$ state, has significant consequences in the band structure, particularly at X point of BZ.²⁴ It will be interesting to perform a complete band structure calculation of $\text{Eu}_{1-x}\text{Ca}_x\text{B}_6$ to see whether the observed band shift is reproduced, and also to find which effect plays the major role of it.³⁴ As for the 1.5 eV peak, Caimi *et al.* assigned it to the intra-atomic Eu $4f \rightarrow 5d$ transitions.^{35,36} This is consistent with the absence of the peak in CaB_6 .

In Fig. 2(b), we show the low-frequency part of the spectrum. The sharp peaks at $\omega \approx 146$ and 858 cm^{-1} represent infrared-active phonons. The rapid increase of $\sigma_1(\omega)$ at low-frequency with decreasing ω represents the metallic response of free carriers. This intraband conductivity decreases with x and is suppressed to a negligible amount for $x \geq 0.35$, indicating that the metallic carriers disappear. We estimate the spectral weight of $\sigma_1(\omega)$ in terms of the plasma frequency ω_p using the relation $\omega_p^2 = \frac{120}{\pi} \int_0^{\omega_c} \sigma_1(\omega) d\omega$. Here the cut-off frequency ω_c for the integration was taken as 2000 cm^{-1} . The phonon contribution was subtracted from the sum. The result is shown in Fig. 4 which will be discussed later. Additionally, we note that the intraband $\sigma_1(\omega)$ does not follow the conventional Drude form. Perucchi *et al.* analyzed it as a sum of several Drude components.³⁷

In EuB_6 , the metallic carrier creation is attributed either to an extrinsic origin such as a boron vacancy²² or to the intrinsic semimetallic CB-VB overlap.²³ Degiorgi *et al.* measured reflectivity of an independent EuB_6 sample.⁴ The plasma edge in that work coincides with ours, suggesting that the carrier density is same. In the present work, the plasma frequency changes systematically in Ca-doped samples. It is less likely that these results come from uncontrolled random vacancies. As for the latter scenario, which seems more plausible at this point, the carrier density depends on the amount of the band overlap at X-point. The x -dependence of ω_p suggests that the overlap decreases with Ca-doping. For $x \geq 0.35$, it is inferred that CB and VB are separated.

To test this picture more directly, let us give a closer

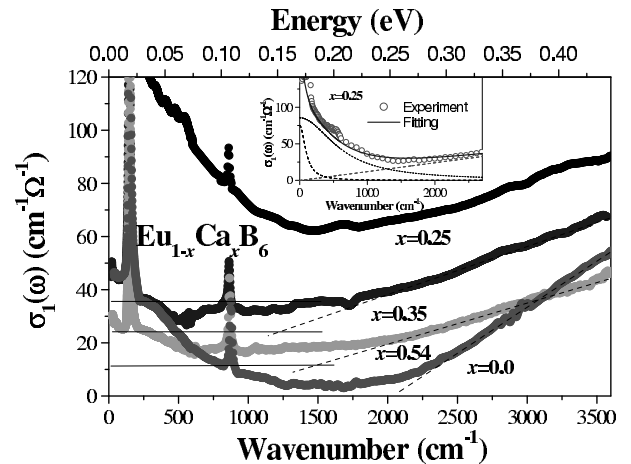


FIG. 3: Optical conductivity of $\text{Eu}_{1-x}\text{Ca}_x\text{B}_6$ below 0.5 eV. The curves are displaced vertically. The solid horizontal lines show the displacements. The dashed lines are used to determine the absorption edge of the interband transition. (Inset): A decomposition of $\sigma_1(\omega)$ of $x = 0.25$ into intraband and interband contributions. We use two Drude conductivities to fit the intraband $\sigma_1(\omega)$. The phonon peak was subtracted from the data.

look at the onset of the interband conductivity which corresponds to the VB-CB excitation at X point. In Fig. 3 we show $\sigma_1(\omega)$ in the mid-infrared region for four samples, one below x_c ($x = 0.25$) and the rest at $x \geq x_c$. For a clearer presentation, the curves have been displaced vertically. The interband $\sigma_1(\omega)$ appears as a linear rise with increasing ω on the high energy side of the spectra. For the samples with $x \geq 0.35$, we extrapolate along the linear region to find the onset energy Δ , as shown by the dashed lines. At $x = 1$ (CaB_6), Δ is about 0.25 eV. The Drude feature in the far-infrared region represents perhaps residual impurity-induced carriers. At $x = 0.54$ and 0.35 , Δ is smaller. For these two samples, Δ determination is somewhat uncertain due to the remnant $\sigma_1(\omega)$ at $\omega < \Delta$.³⁸ At $x = 0.25$, the intraband $\sigma_1(\omega)$ is strong. Various model functions fit to the intraband $\sigma_1(\omega)$ were evaluated, but depending on the fitting details, Δ varied from 0 to as large as 0.2 eV. The inset illustrates a fit with $\Delta = 0$ which corresponds to the case where the bands overlap. The large uncertainty of Δ makes it difficult to determine the X-point band state for $x < 0.35$.

In Fig. 4, we summarize the observed optical changes of the 2.7 eV peak position Ω , the squared plasma frequency ω_p^2 and the interband onset frequency Δ . The Ω in CaB_6 ($=3.35 \text{ eV}$) is about 0.6 eV higher than in EuB_6 . Meanwhile, the band overlap in EuB_6 estimated from the band calculation is about 0.3 eV.²⁴ If the bands move rigidly throughout the BZ, the X-point separation at $x = 1$ will be 0.3 eV. This is close to the observed $\Delta = 0.25 \text{ eV}$ of CaB_6 . Also the bands will fall apart ($\Delta = 0$) when the shift is 0.3 eV. This occurs, from Fig.4(a), at $x = 0.35$, which agrees with the suppression of ω_p^2 . However, Δ at this composition ($= 0.15 \text{ eV}$) is rather significant. It

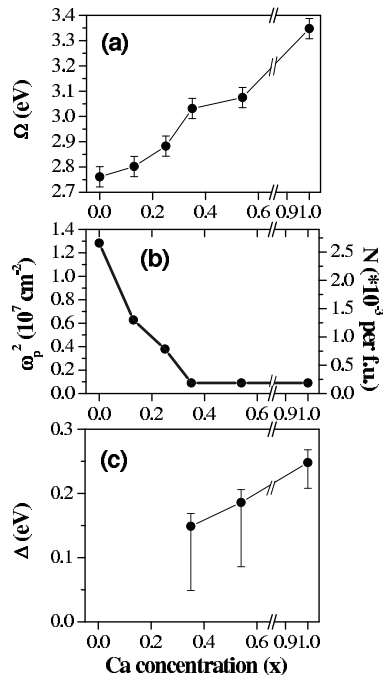


FIG. 4: The changes of the optical features of $\text{Eu}_{1-x}\text{Ca}_x\text{B}_6$ with x . (a) Position of the 2.7 eV peak. (b) Squared plasma frequency ω_p^2 (c) Absorption onset of the interband transition. In (b), ω_p^2 is converted into carrier density n (right axis) from $\omega_p^2 = 4\pi n e^2 / m^*$ using $m^* = 0.25$ [ref.18 and 19]. Error bars of the values are indicated together.

may indicate that the gap opens quickly, i.e, between $x = 0.25$ and 0.35 , the band shift at the X-point occurs faster than the other part of x . Interestingly, the change of Ω shows a rapid shift for this x range. However, due to the uncertainty of Δ at $x = 0.35$, it is difficult to draw the exact x -dependence of the gap opening. Nevertheless, the overall behaviors of the three optical conductivity features show consistently that the electronic structure transition occurs from the semimetallic EuB_6 to the insulating CaB_6 through the band shift. EuB_6 exhibits

a ferromagnetic transition at $T_c = 15$ K. It was found that T_c decreases with Ca-substitution and then, interestingly, disappears at x_c . This correlation suggests that the ferromagnetism is coupled with the charge carrier.³⁹ A quantitative analysis of this relationship will be discussed in an independent paper.⁴⁰

In summary, we have performed reflectivity and ellipsometry measurements on the isovalent hexaboride series compounds $\text{Eu}_{1-x}\text{Ca}_x\text{B}_6$ ($0 \leq x \leq 1$) over wide energy range of 2.5 meV - 6 eV and found that the optical conductivity exhibits systematic evolutions from EuB_6 to CaB_6 . The interband $\sigma_1(\omega)$ including the two peaks at 2.7 eV and 3.7 eV shifts continuously to higher energy as x increases. This shows that, along with the cation substitution, the valence band and the conduction band move away from each other throughout the Brillouine zone and the VB to CB energy distance increases with the Ca-content. As for the the low-frequency intraband $\sigma_1(\omega)$, the Drude spectral weight decreases continuously with x and suppressed for $x > 0.35$. In EuB_6 , we adopted the semimetallic band structure calculation results and showed that the observed behaviors of the low frequency $\sigma_1(\omega)$ are most readily explained in terms of the band shift at the X point of BZ. The carrier density decreases due to the decrease of the CB-VB overlap. At higher x , the two bands are separated to open a band gap, which is consistent with the optical absorption onset at finite frequency, 0.25 eV in CaB_6 . As we mentioned in the introduction, extensive efforts have been made to calculate the band structure of EuB_6 and CaB_6 . The observations of the present work, i.e, the systematic evolution of the electronic structure along with the cation substitution in $\text{Eu}_{1-x}\text{Ca}_x\text{B}_6$ provide a strong constraint on the band structure calculations and should guide future works toward the complete understanding of the hexaboride compounds.

This work was supported by the KRF Grant No. 2002-070-C00032 and the KOSEF through CSCMR. Work at Brookhaven National Laboratory was supported by the DOE under Contract No. DE-AC02-98CH10886.

¹ B. T. Matthias, T. H. Geballe, K. A. adn E. Corenzwit, G. W. Hull, and J. P. Maita, *Science* **159**, 530 (1968).
² M. Kasaya, J. M. Tarascon, J. Etourneau, and P. Hagenmuller, *Mater. Res. Bull.* **13**, 1055 (1978).
³ Z. Fisk, D. C. Johnston, B. Cornut, S. von Molnar, S. Oseroff, and R. Calvo, *J. Appl. Phys.* **50**, 1911 (1979).
⁴ L. Degiorgi, E. Felder, H. R. Ott, J. L. Sarrao, and Z. Fisk, *Phys. Rev. Lett.* **79**, 5134 (1997).
⁵ S. Broderick, B. Ruzicka, L. Degiorgi, H. R. Ott, J. L. Sarrao, and Z. Fisk, *Phys. Rev. B* **65**, 121102 (2002).
⁶ D. P. Young, D. Hall, M. E. Torelli, Z. Fisk, J. L. Sarrao, J. D. Thompson, H. R. Ott, S. B. Oseroff, R. G. Goodrich, and R. Zysler, *Nature (London)* **397**, 412 (1999).
⁷ M. E. Zhitomirsky, T. M. Rice, and V. I. Anisimov, *Nature*

(London) **402**, 251 (1999).

⁸ L. Balents and C. M. Varma, *Phys. Rev. Lett.* **84**, 1264 (2000).
⁹ V. Barzykin and L. P. Gorkov, *Phys. Rev. Lett.* **84**, 2207 (2000).
¹⁰ S. Murakami, R. Shindou, N. Nagaosa, and A. S. Mishchenko, *Phys. Rev. Lett.* **88**, 126404 (2002).
¹¹ S. Murakami, R. Shindou, N. Nagaosa, and A. S. Mishchenko, *Phys. Rev. B* **66**, 184405 (2002).
¹² D. Ceperley, *Nature (London)* **397**, 386 (1999).
¹³ G. Ortiz, M. Harris, and P. Ballone, *Phys. Rev. Lett.* **82**, 5317 (1999).
¹⁴ J. L. Gavilano, S. Mushkolaj, D. Rau, H. R. Ott, A. Bianchi, D. P. Young, and Z. Fisk, *Phys. Rev. B* **63**,

- 140410 (2001).
- ¹⁵ K. Matsubayashi, M. Maki, T. Moriwaka, T. Tsuzuki, T. Nihoka, C. H. Lee, A. Yamamoto, T. Ohta, and N. Sato, *J. Phys. Soc. Jpn.* **72**, 2097 (2003).
 - ¹⁶ K. Matsubayashi, M. Maki, T. Tsuzuki, T. Nihoka, and N. K. Sato, *Nature (London)* **420**, 143 (2002).
 - ¹⁷ D. P. Young, Z. Fisk, J. D. Thompson, H. R. Ott, S. B. Oseroff, and R. G. Goodrich, *Nature (London)* **420**, 144 (2002).
 - ¹⁸ R. G. Goodrich, N. Harrison, J. J. Vuillemin, A. Teklu, D. W. Hall, Z. Fisk, D. Young, and J. Sarrao, *Phys. Rev. B* **58**, 14896 (1998).
 - ¹⁹ M. C. Aronson, J. L. Sarrao, Z. Fisk, M. Whitton, and B. L. Brandt, *Phys. Rev. B* **59**, 4720 (1999).
 - ²⁰ T. Terashima, C. Terakura, Y. Umeda, N. Kimura, H. Aoki, and S. Kunii, *J. Phys. Soc. Jpn.* **69**, 2423 (2000).
 - ²¹ D. Hall, D. P. Young, Z. Fisk, T. P. Murphy, E. C. Palm, A. Teklu, and R. G. Goodrich, *Phys. Rev. B* **64**, 233105 (2001).
 - ²² J. D. Denlinger, J. A. Clack, J. W. Allen, G.-H. Gweon, D. M. Poirier, C. G. Olson, J. L. Sarrao, A. D. Bianchi, and Z. Fisk, *Phys. Rev. Lett.* **89** (2002).
 - ²³ S. Massidda, A. Continenza, T. M. D. Pascale, and R. Monnier, *Z. Phys. B* **102**, 83 (1997).
 - ²⁴ J. Kuneš and W. E. Pickett, *Phys. Rev. B* **69**, 165111 (2004).
 - ²⁵ H. J. Tromp, P. van Gelderen, P. J. Kelly, G. Brocks, and P. A. Bobbert, *Phys. Rev. Lett.* **87**, 016401 (2001).
 - ²⁶ C. O. Rodriguez, R. Weht, and W. E. Pickett, *Phys. Rev. Lett.* **84**, 3903 (2000).
 - ²⁷ Z. Wu, D. J. Singh, and R. E. Cohen, *Phys. Rev. B* **69**, 193105 (2004).
 - ²⁸ H. Kino, F. Aryasetiawan, K. Terakura, and T. Miyake, *Phys. Rev. B* **66**, 121103(R) (2002).
 - ²⁹ M. van Schilfgaarde and T. Kotani, (unpublished).
 - ³⁰ J.-S. Rhyee, B. K. Cho, and H.-C. Ri, *Phys. Rev. B* **67**, 125102 (2003).
 - ³¹ J.-S. Rhyee, B. H. Oh, B. K. Cho, H. C. Kim, and M. H. Jung, *Phys. Rev. B* **67**, 212407 (2003).
 - ³² C. C. Homes, M. Reedyk, D. A. Crandles, and T. Timusk, *Appl. Opt.* **32**, 2976 (1993).
 - ³³ A. Hasegawa and A. Yanase, *J. Phys. C* **12**, 5431 (1979).
 - ³⁴ In fact, in Ref. 23, the authors calculated the band structure of EuB_6 and CaB_6 using the LDA method.²³ The result shows that the VB-CB distance at Γ point is smaller in CaB_6 by about 0.5 eV, contrary to the observation.
 - ³⁵ G. Caimi, S. Broderick, H. R. Ott, L. Degiorgi, A. D. Bianchi, and Z. Fisk, *Phys. Rev. B* **69**, 012406 (2004).
 - ³⁶ P. Vonlanthen, E. Felder, L. Degiorgi, H. R. Ott, D. P. Young, A. D. Bianchi, and Z. Fisk, *Phys. Rev. B* **62**, 10076 (2000).
 - ³⁷ A. Perucchi, G. Caimi, H. R. Ott, L. Degiorgi, A. D. Bianchi, and Z. Fisk, *Phys. Rev. Lett.* **92**, 067401 (2004).
 - ³⁸ We have confirmed that $\sigma_1(\omega)$ in this energy range is insensitive to the low frequency extrapolation of the Kramers-Kronig transformation.
 - ³⁹ J.-S. Rhyee, B. H. Oh, B. K. Cho, M. H. Jung, H. C. Kim, K. Yoon, J. H. Kim, and T. Ekino, cond-mat/0310068.
 - ⁴⁰ Jungho Kim and Eunjip Choi (unpublished).